
Steering a virtual blowfly: simulation of visual pursuit

Norbert Boeddeker* and Martin Egelhaaf

Department of Neurobiology, Bielefeld University, PO Box 10 01 31, 33501 Bielefeld, Germany

The behavioural repertoire of male flies includes visually guided chasing after moving targets. The visuo-motor control system for these pursuits belongs to the fastest found in the animal kingdom. We simulated a virtual fly, to test whether or not experimentally established hypotheses on the underlying control system are sufficient to explain chasing behaviour. Two operating instructions for steering the chasing virtual fly were derived from behavioural experiments: (i) the retinal size of the target controls the fly's forward speed and, thus, indirectly its distance to the target; and (ii) a smooth pursuit system uses the retinal position of the target to regulate the fly's flight direction. Low-pass filters implement neuronal processing time. Treating the virtual fly as a point mass, its kinematics are modelled in consideration of the effects of translatory inertia and air friction. Despite its simplicity, the model shows behaviour similar to that of real flies. Depending on its starting position and orientation as well as on target size and speed, the virtual fly either catches the target or follows it indefinitely without capture. These two behavioural modes of the virtual fly emerge from the control system for flight steering without implementation of an explicit decision maker.

Keywords: vision; sensorimotor control; fly; chasing; model; smooth pursuit

1. INTRODUCTION

Male flies chase moving targets in fast acrobatic flights. If the target is caught and turns out to be a conspecific female, the flies possibly mate (Land & Collett 1974; Wehrhahn *et al.* 1982; Wagner 1986). The goal of our investigations is to comprehensively understand the functioning of the system controlling the virtuosic pursuit behaviour. In a first step towards this goal we analysed chasing behaviour experimentally (Boeddeker *et al.* 2003). In the present account we compare the behavioural performance of real flies with the performance of a virtual fly which incorporates our experimentally established hypotheses for the control system underlying chasing.

The blowfly *Lucilia* is our experimental animal, because it is amenable to behavioural and neurophysiological techniques. We performed a behavioural systems analysis using a black sphere instead of real flies as target, which was moved on a circular track in a small flight arena (Boeddeker *et al.* 2003). By this approach it has been possible to systematically control and manipulate the visual input of the pursuing fly, even under free-flight conditions. The main findings were as follows: (i) the chasing fly keeps the retinal position of the target in the frontal field of view by smooth rotation about the vertical head axis; (ii) depending on the size and the speed of the target, the fly exhibits one of two chasing modes: the target is either caught after relatively short pursuit flights or followed by the chasing fly for up to several seconds on precisely controlled tracks without being caught; and (iii) during such 'unsuccessful' chases, the fly follows a large target at a greater distance than a small target. In this way the retinal size of the target is kept approximately constant during pursuit, irrespective of its absolute size. However, the retinal size at which the target is followed decreases with increasing target speed.

Pursuit behaviour in flies has already been modelled at different levels of explanation, ranging from phenomenological models (Land & Collett 1974; Reichardt & Poggio 1976) to neuronal network models (Missler & Kamangar 1995). The latter model was inspired by the anatomy of the fly's visual system and general properties of fly visual interneurons. All these models focus on the visual control of flight direction which enables the chasing fly to fixate the target in the frontal field of view but omit the control of forward velocity. The artificial hoverfly developed by Cliff (1992) comprises not only a neural network controller performing foveal fixation of a target, but additionally contains a network that regulates the distance to the target. This artificial hoverfly was based on hypotheses on visual flight control mechanisms in *Syrirta pipiens* (Collett & Land 1975). A similar approach was taken in a recent study (Anderson & McOwan 2003) implementing a computational model of a stealth strategy inspired by the apparent mating tactics of male hoverflies (Srinivasan & Davey 1995).

None of these pursuit models is designed to explain the chasing behaviour of *Lucilia* and, in particular, its two chasing modes. This is accomplished by the virtual blowfly introduced here. Another feature of our virtual blowfly, not taken into account in previous pursuit models, is the simulation of the effects of translatory inertia and air friction on locomotion.

We use a minimal set of operating instructions to generate fly-like chasing behaviour. One might think of two separate control systems underlying chasing behaviour in *Lucilia*: one mediating pursuit before capture and one for the guidance of target capture. However, our behavioural analysis suggests that both behavioural components can be explained parsimoniously as the consequence of a single control system for speed control. We suppose that the control system is tweaked to steer a flight course resulting in the capture of targets of proper size and speed, i.e. the size and speed of female *Luciliae*. The real and the virtual

*Author for correspondence (norbert.boeddeker@uni-bielefeld.de).

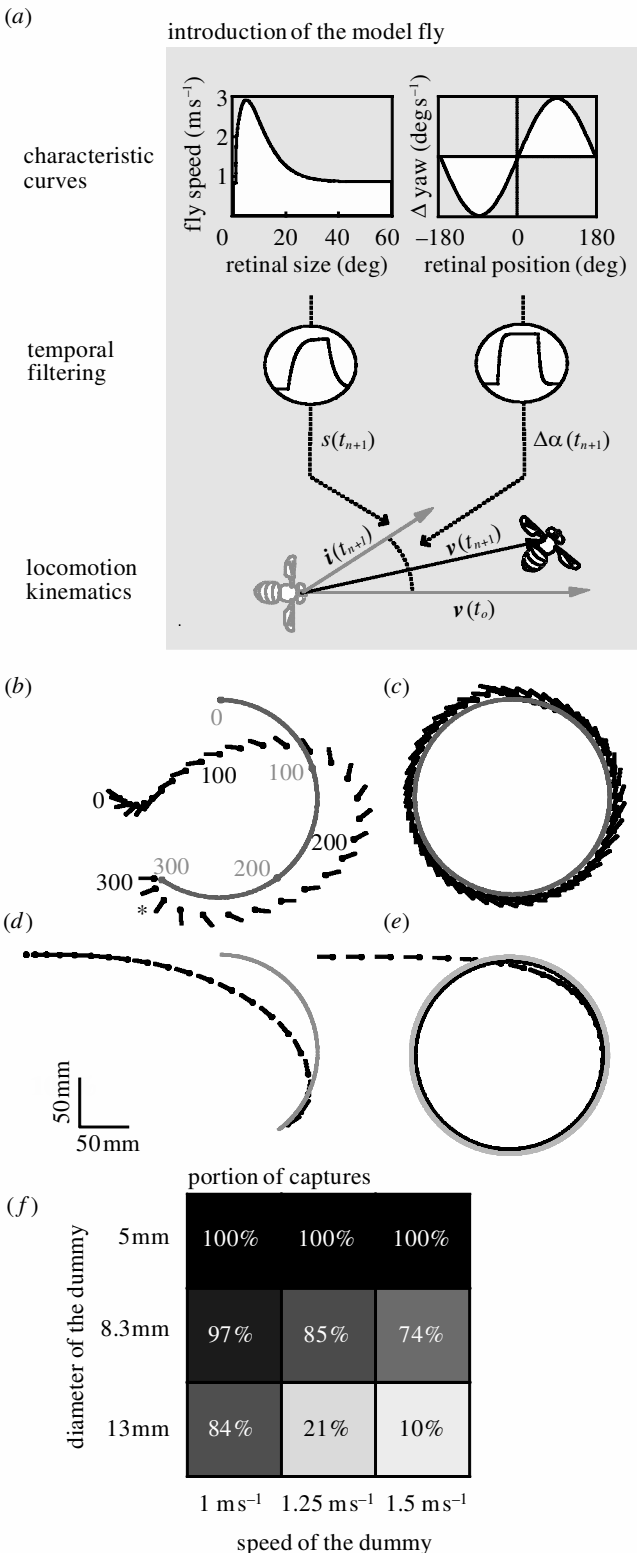


Figure 1. (a) Layout of the virtual fly. The output of the virtual fly's speed controller (pathway on the left) depends on retinal target size and determines the absolute value of the fly's speed vector for the next simulation step ($s(t_{n+1})$). The fixation controller (pathway on the right), converts in each simulation step the error angle into angular speed of the pursuing virtual fly ($\Delta\alpha(t_{n+1})$). First-order low-pass temporal filters are applied to the outputs of both visual pathways mimicking neuronal processing and muscular reaction time. The filtered outputs from each pathway form the 'intended' vector ($\mathbf{i}(t_{n+1})$) of locomotion of the virtual fly. A third module emulates the kinematics of fly body movements and determines the virtual fly's velocity in the next simulation step ($\mathbf{v}(t_{n+1})$) as the weighted sum of the actual fly velocity $\mathbf{v}(t_n)$ and the 'intended' velocity vector. (b) Example of a simulated C chase. Trajectory of a fly (black markers) capturing the target (grey markers). The virtual fly is indicated by the position of its centroid (circle) and the orientation of the body axis (line) every 10 ms. The numbers denote corresponding positions of the fly and the target every 100 ms. The asterisk denotes a sudden turn of the fly, before it catches the target. (c) Example of a simulated pursuit of the target without capture (P chase). (d) An unrealistic flight trajectory with a virtual fly that is not affected by viscous air damping or inertia (M in equation (2.3) is set to 1). (e) The same virtual fly as shown in (d) but additionally τ_v is set to zero which will always result in endless pursuit without target capture. (f) Dependence of target capture on target size and target speed. The virtual fly was started from 441 different positions and from each position with four different body axis orientations. The target was either caught after short pursuits (see (b)) or followed indefinitely without capture (see (c)) until the simulation was stopped. The percentage gives the portion of captures among all chases for a given combination of target parameters.

flying altitude. Rotations of the head relative to the surroundings around the pitch and roll axes are generally small during flight (Schilstra & Van Hateren 1998). Therefore, we restricted the mobility of our virtual fly to rotation about its vertical axis and to translation in the horizontal plane, with gaze direction being equivalent to body orientation. These three degrees of freedom are sufficient to enable the virtual fly to generate those steering behaviours we found in real flies chasing a dummy target on a circular track.

We implemented two visual pathways in our virtual fly: one for target fixation (figure 1a, right) and one for speed control (figure 1a, left). Whereas the retinal size of the target controls the forward speed of the virtual fly, the position of the retinal image of the target determines the fly's flight direction. First-order low-pass temporal filters are applied to the outputs of both visual pathways, mimicking neuronal processing and muscle reaction time. In accordance with our experimental results, the time constant in the target fixation pathway was 15 ms, and thus much shorter than the time constant of the pathway for speed control (80 ms). The outputs from each pathway form the 'intended' vector of locomotion of the virtual fly, as it is represented at its motor output. However, as a consequence of friction and inertia, this intended vector of locomotion does not exclusively determine the actual trajectory of the virtual fly. A third module emulates the kinematics of fly body movements and determines the

fly can be deluded if the target is either larger or faster than conspecifics.

2. DESIGN OF THE VIRTUAL FLY

In our behavioural experiments, chasing flies mainly moved in a plane below and parallel to the plane in which the target moved (Boeddeker *et al.* 2003). This feature was particularly obvious for extra-long chases without target capture, during which chasing flies rarely varied their

virtual fly's actual position and orientation in the next simulation step. Data are updated 1000 times per simulated second.

(a) Speed control

Viewed from the pursuer's position, the image of the target subtends a visual angle ρ ('retinal size'). The retinal size depends on the absolute size of the target and on the distance between pursuer and target. Our behavioural analysis revealed a systematic relation between absolute target size and the distance the fly keeps to the target during non-capture chases (Boeddeker *et al.* 2003). As a consequence, the retinal size is almost constant for a given target speed, independent of the absolute target size. Therefore, the output of the virtual fly's speed controller (s) was assumed to depend on retinal target size (ρ). Male *Luciliae* follow a fast moving target at a larger distance and thus see it at a smaller retinal size than a slowly moving target (Boeddeker *et al.* 2003). Therefore, we assumed the output of the speed controller to decrease with increasing retinal target size. Because the spatial resolution of eyes is limited, we defined a lower angular size limit for target perception. If the angular size of a target is 0.5° or smaller the controller output is not affected by target size but adjusted to a 'spontaneous' speed ' S_g '. The relationship between the retinal size of the target and the output of the speed controller is given by the following equation with model parameters S_g , S_v and ρ^* . The location of the maximum of the speed controller's characteristic curve is given by ρ^* . The parameter S_v determines the gain for velocity control.

$$s(t_{n+1}) = \begin{cases} S_g & \text{if } \rho \leq 0.5^\circ \\ \rho(t_n) S_v e^{-\rho(t_n)/\rho^*} + S_g & \text{if } \rho > 0.5^\circ \end{cases} \quad (2.1)$$

(b) Target fixation

The angle subtended by the fly's longitudinal body axis and the line connecting the fly with the target represents the deviation of the target position from the frontal midline of the pursuer's head ('error angle'). The error angle is defined in a fly-centred polar coordinate system with 0° pointing directly ahead. A fixation controller, converting in each simulation step the error angle (ϕ) into angular speed of the pursuing virtual fly in the horizontal plane ($\Delta\alpha$), can be formalized by equation (2.2):

$$\Delta\alpha(t_{n+1}) = \begin{cases} 0 & \text{if } \rho \leq 0.5^\circ \\ G \sin(\phi(t_n)) & \text{if } \rho > 0.5^\circ \end{cases} \quad (2.2)$$

G determines the gain of the orientation change. It is zero if the retinal size of the target is smaller than 0.5° . To compute the orientation of the virtual fly in the next simulation step ($\alpha(t_{n+1})$) the low-pass filtered output of the fixation controller ($\Delta\alpha(t_{n+1})$) is added to $\alpha(t_n)$, i.e. the orientation in the previous time-step. Given the small size of a fly its angular momentum can be neglected (Land & Collett 1974; Reichardt & Poggio 1976).

(c) Virtual fly kinematics

To steer the fly, the output signals of the fixation and speed controllers are used to compute one vector for each simulation step: the intended velocity (\mathbf{i}). The direction

of this vector is determined by the fixation controller, its length by the speed controller. In the physical world the fly's locomotion depends on the ratio between maximum force production and body inertia, which affects the maximum occurring accelerations of the fly. The locomotor capacity of a fly is also affected by viscous air damping and gravity. A velocity change in real flies is the result of the above-described forces acting on the fly's body. These forces cannot be directly measured in free-flight experiments. We therefore follow an approach that has been used to steer autonomous agents in computer animations (Reynolds 1999). Treating the virtual fly as a point mass, its kinematics are modelled by the computationally cheap forward Euler integration. For each simulation step the new velocity vector \mathbf{v} is given by the following formula:

$$\mathbf{v}(t_{n+1}) = (1 - M)\mathbf{v}(t_n) + M\mathbf{i}(t_{n+1}) \quad (2.3)$$

with $0 < M < 1$.

To what extent the intended velocity determines the virtual fly's trajectory and the trajectory is predetermined by the preceding flight path can be adjusted by the parameter M . M was used to fit the shape of the virtual fly's trajectories until they looked similar to those of real flies. Adding the 'new' velocity vector to the 'old' fly position results in the position of the virtual fly in the next simulation step; the direction of \mathbf{i} corresponds to the gaze direction (figure 1a, bottom).

In accordance with our behavioural experiments, the simulated targets (sizes: 5 mm, 8.3 mm and 13 mm) were moved on a circular track (radius: 100 mm, speeds: 1 m s^{-1} , 1.25 m s^{-1} and 1.5 m s^{-1}), always starting from the same position. The virtual fly was released from 441 evenly distributed starting positions in a simulated $300 \text{ mm} \times 300 \text{ mm}$ square sized flight arena. At each start position the virtual fly started with the spontaneous velocity (0.8 m s^{-1}) at four different angles (0° , 90° , 180° , 270°) of gaze direction. When the virtual fly came closer to the target than the target radius plus 5 mm, which corresponds approximately to the length of the fly's legs, we assumed that the target was caught and the simulation was terminated.

3. RESULTS

(a) Adjustment of model parameters

The behaviour of the virtual fly can be manipulated by variation of seven parameters: the two first-order low-pass filter time constants acting on fixation (τ_f) and speed control (τ_v), the gain of yaw rotation (G), the movement coefficient (M), and three parameters characterizing the transfer function of the speed controller (S_g , S_v , ρ^*). We adjusted these parameters within the constraints set by our behavioural analysis (Boeddeker *et al.* 2003): (i) the speed of blowflies does not exceed 3 m s^{-1} or fall below 0.25 m s^{-1} ; and (ii) the time constants in the fixation (τ_f) and speed controller (τ_v) were set to 15 ms and 80 ms, respectively. The gain for yaw rotation ($G = 0.125$) was adapted to produce stable fixation behaviour and to prevent the rotational speed from exceeding $5000^\circ \text{ s}^{-1}$. To obtain realistic trajectories M was set to 0.0455. M values near 1 would mimic an unrealistic fly that is not affected by viscous air damping or inertia (figure 1d). The time

constant of the low-pass filter in the speed branch (τ_v) must be non-zero to enable the virtual fly to catch the target. Setting τ_v to zero and M to 1 will always result in endless pursuit without target capture (figure 1e). Capture behaviour (figure 1b) is strongly related to the parameters of speed control, which we parameterized with $S_g = 0.8 \text{ m s}^{-1}$, $S_v = 67$ and $\rho^* = 0.0865$. It should be noted that the qualitative features of the virtual fly's behaviour are very robust to variations of most of these parameters. We chose a set of parameters that leads to results qualitatively similar to those obtained in behavioural experiments on real flies, as regards the percentage of target captures and the shape of trajectories. Parameterized in this manner, the virtual fly was tested to determine whether or not it also reproduced other aspects of chasing behaviour we characterized in behavioural experiments.

(b) *Performance of the virtual fly in explaining behavioural results*

For a given target size and speed, small variations in the virtual fly's starting position and orientation can determine whether or not the target is caught. When we tested the virtual fly from different starting positions with different body axis angles the target was either caught after short pursuits (example in figure 1b) or followed indefinitely without capture (figure 1c) until the simulation was stopped. In analogy to the behavioural experiments, simulated chasing flights can therefore be classified into two categories: capture flights (C chases) and pursuit flights without capture (P chases). The probability of target capture depends on target size and speed (figure 1f) in qualitatively the same way as found in real flies (Boeddeker *et al.* 2003). Targets much larger than a real fly were chased, but were only seldom caught. Fly-sized targets (5 mm) were caught more often than larger targets. This holds true for all tested target speeds, although with increasing target speed, the frequency of capture decreases.

While chasing the target on its circular track, the fly continuously changes the orientation of its body long axis to keep the target centred in the frontal part of the visual field (figure 2a). Despite the fact that we built a continuous controller, occasionally rapid saccade-like turns occur, identifiable by a brief rotational velocity peak. These go along with rapid body orientation changes. Saccade-like turns occur, at the beginning of a chase (figure 2a, arrow), when the virtual blowfly approaches the target very closely but misses it (P chases, not shown), or shortly before capture in C chases (figure 1b, asterisk). A more detailed analysis of saccades during chasing behaviour will be presented in a subsequent paper. In P chases the virtual blowfly will reach a steady state after some time with respect to its angular velocity and retinal error angle (figure 2a).

The error angle is constant during the steady state of P chases and the mean rotational velocity of the virtual blowfly exactly equals the rotational velocity of the target after several seconds (figure 2c, vertical lines on the x -axis; values: 573° s^{-1} , 716° s^{-1} , 859° s^{-1}). The value of the steady-state retinal error is slightly shifted in the direction in which the target would move on the eye if it were not fixated. The error slightly increases with increasing target speed (figure 2b, vertical lines on the x -axis; values: 4.5° , 5.75° , 6.9°). In C chases qualitatively the same dependence

on target velocity is found for the error angle and the yaw velocity as in P chases. However, in contrast to the steady state of P chases, the distributions of the error angle (figure 2b) and the yaw velocity (figure 2c) are broad. This is mainly a consequence of geometry: unless the fly is not directly heading towards the target, the error angle will, on average, increase the more for a given translational movement the closer the virtual fly is to the target. Because the error angle is the signal that drives rotational velocity, larger turns are likely to occur if the virtual fly is close to the target (e.g. figure 1b, asterisk). The time-lag between retinal error angle and the fly's rotational velocity, as determined by cross-correlation, is -12 ms (figure 2d). Periodicity in the cross-correlograms results from oscillation of the underlying fixation controller.

After the onset of P chases, the retinal size at which the target is seen by the virtual fly and, accordingly, the translational velocity which is controlled by it, tend to oscillate until they settle to a steady-state level (figure 3a). In the steady state, the retinal target size is independent of the absolute target size (figure 3c) implying that larger targets are followed at a larger distance than smaller ones. However, retinal target size decreases with increasing target velocity (figure 3c). These features of the virtual blowfly's behaviour agree well with the performance of its biological counterpart (Boeddeker *et al.* 2003). Because in C chases the target is eventually caught, the retinal size inevitably increases during an approach. The speed of the virtual fly initially increases above target speed, but it slows down when the retinal target size gets too large just before catching the target (figure 3b). The time-lag of *ca.* -75 ms between the retinal target size and the blowfly's speed, as determined by cross-correlation, can be attributed to the locomotion kinematics of the virtual fly and the simulated neuronal processing time-lag of the speed controller (figure 3d). This time-lag is, in accordance with our experimental results (Boeddeker *et al.* 2003), shorter than the time-lag for fixation control.

4. DISCUSSION

We propose a chasing controller for a virtual blowfly that is able to chase moving targets with an efficiency similar to that of real flies. Following the principle of parsimony, we built this virtual blowfly as simply as possible. The virtual blowfly is equipped with two visual control systems for steering motor actions, one that controls flight speed, depending on retinal target size, and another that mediates turns depending on the location of the target in the visual field. It turned out to be relevant for the proper performance of the virtual blowfly to take into account time-lags due to neuronal processing as well as the locomotion kinematics of blowflies. Most important, the virtual blowfly shows a bifurcation into two behavioural modes similar to real blowflies: the target is either caught (C chases) or pursued without capture (P chases). Such a dual response mode comes about without assuming an explicit decision maker. Chasing behaviour of blowflies as one of the most virtuosic visually guided behaviours found in the animal kingdom might therefore be regarded as an example of complex behaviour that emerges from simple rules.

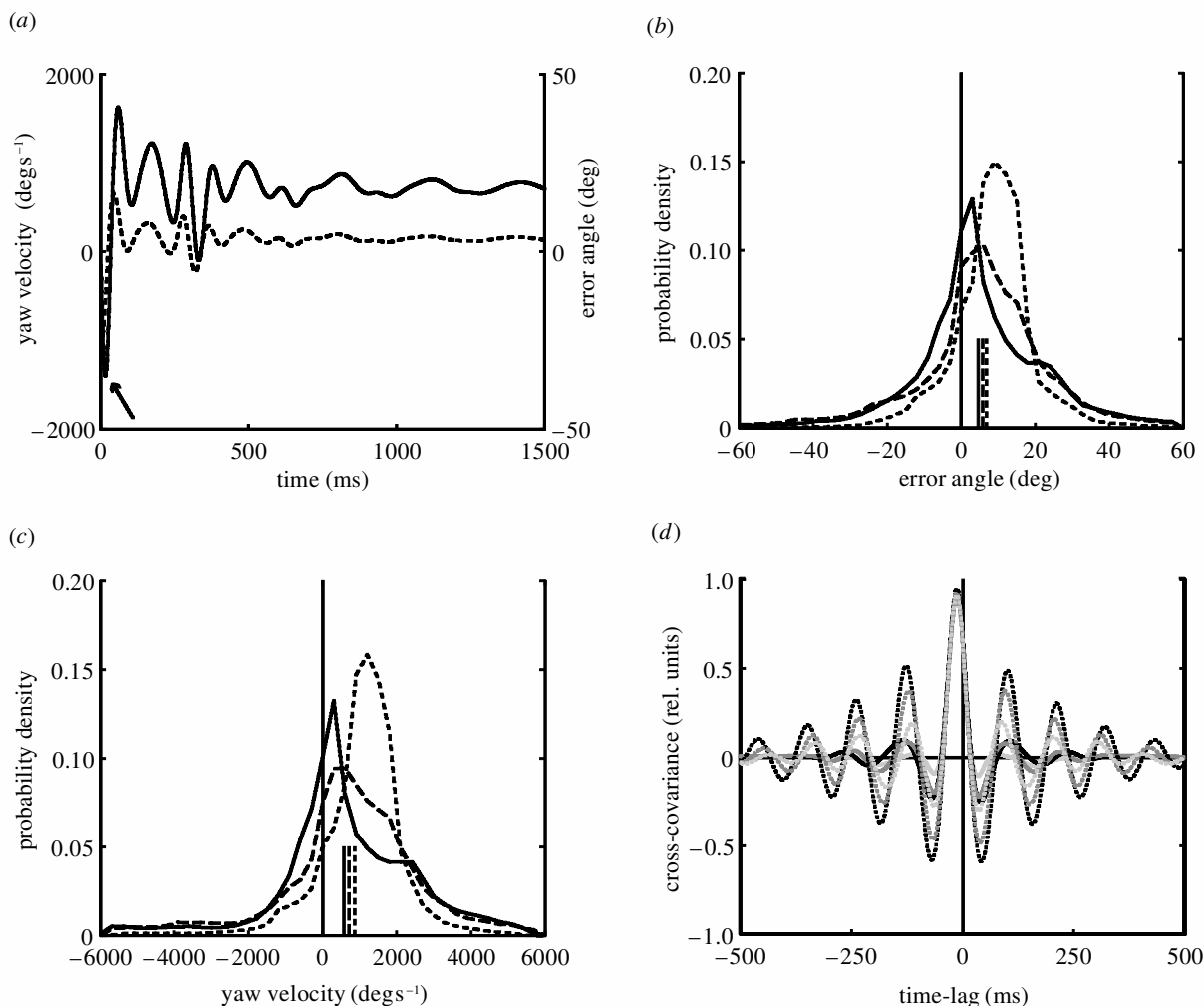


Figure 2. Control of yaw rotation. (a) Rotational velocity of a fly (solid line) and error angle of the target (dotted line) during the first 1500 ms of the P chase example shown in figure 1c. (b) Probability density of the error angle for C chases. The steady-state error angles during P chases after targets of different speeds are indicated by lines on the x -axis by the same linestyles for different target speeds as for C chases. Solid line, 1 m s^{-1} ; dashed line, 1.25 m s^{-1} ; dotted line, 1.5 m s^{-1} . (c) Probability density of the yaw velocity for all C chases grouped by target speed (solid line, 1 m s^{-1} ; dashed line, 1.25 m s^{-1} ; dotted line, 1.5 m s^{-1}). A target moving at 1 m s^{-1} on the circular track changes its yaw orientation with 573° s^{-1} (1.25 m s^{-1} and 1.5 m s^{-1} are equivalent to 716° s^{-1} and 859° s^{-1} , respectively). In the steady state of P chases the mean rotational velocity of the virtual blowfly exactly equals that of the target (lines). (d) Mean cross correlation of error angle and yaw velocity during the first 1500 ms of P chases after the 13 mm (solid lines) and 8.3 mm (dotted lines) sized targets. The black lines indicate a target speed of 1 m s^{-1} (dark-grey, 1.25 m s^{-1} ; pale-grey, 1.5 m s^{-1}).

(a) Differences between the behaviour of virtual and real blowflies: limitations of the model

Real flies show much variability at all levels of information processing (reviews in Juusola *et al.* 1996; Warzecha & Egelhaaf 2001). None the less, the proposed virtual blowfly was implemented without internal noise sources. Thus, its behaviour is entirely deterministic. The variability in chasing performance, even for a given size and speed of the target (figure 1f), results only from the variation of starting positions and orientations of the fly relative to the target. If noise sources were inserted into the virtual blowfly, the simulated catching probabilities may well match the experimentally measured probabilities even in quantitative detail. Additionally, a realistic simulation of motion blur, which occurs in the blowfly's retina as a consequence of the temporal properties of its photoreceptors, would impair visual acuity for moving targets of small retinal size (Juusola & French 1997; Korenberg *et al.* 1998). The capture probabilities, especially of small

targets, might then be lower than without taking motion blur into account.

Because, so far, the virtual blowfly is completely deterministic and entirely driven by its sensory input, it will pursue every target of appropriate size in its range of sight. Hence, the model can be expected to match the chasing behaviour of a real blowfly that is 'motivated' to chase. For instance, chasing in flies younger than 5 days occurs very seldom even if a target of appropriate size is present (own observation). Moreover, the 'motivation' to pursue a target may change during a pursuit manoeuvre, for instance if it is unsuccessful for some time. By contrast, during P chases the virtual blowfly will follow the target forever, because changes in 'motivation' were not modelled.

Very little is still known about the flight motor of blowflies. Additionally, the unsteady aerodynamics of insect flight complicate a realistic simulation of the virtual blowfly's trajectories (Dickinson *et al.* 1999; Ellington 1999).

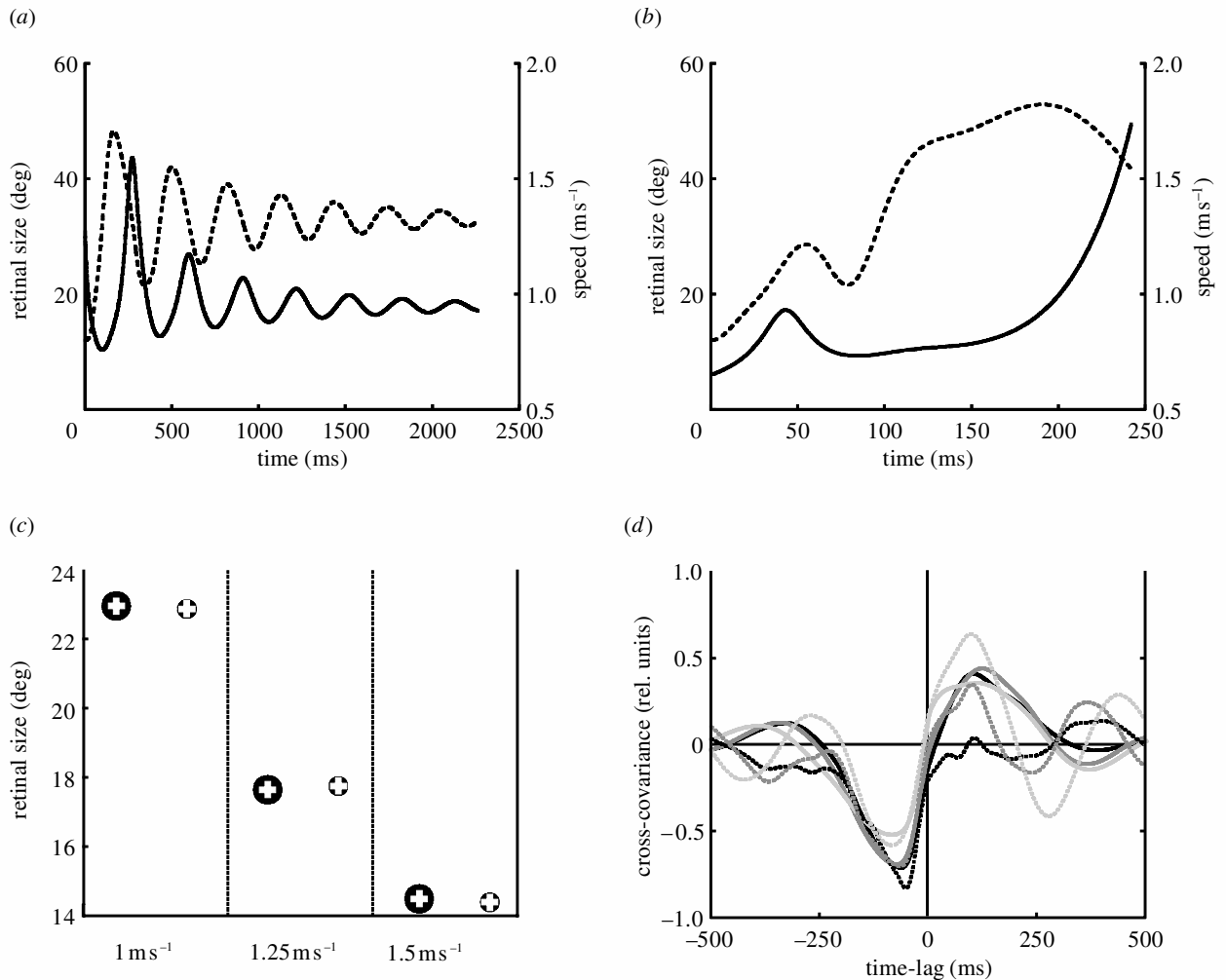


Figure 3. Control of forward speed. (a) Retinal size (solid line) and speed of the fly (dashed line) during the P chase shown in figure 1c. The same variables from the C chase shown in figure 1b are plotted in (b). (c) The retinal size (visual angle) at which the target is seen by the virtual fly settles to a steady-state level during P chases (see (a)). The steady-state retinal size in P chases is independent of the absolute target size (small symbols, 8.3 mm; large symbols, 13 mm) for a given speed. Targets of 5 mm size were always captured (see figure 1f). (d) Cross-correlation between retinal size and fly speed for P chases, plotted as in figure 2d.

Because our intention was to test *visual mechanisms* underlying flight control, we refrained from simulating flight dynamics and used a comparatively computationally cheap kinematic locomotion model.

(b) Relationship to other models of pursuit behaviour

(i) Control of rotation

A principal task of pursuit systems is to minimize the angular error between the actual and the desired retinal position of a target. Formalisms describing pursuit of moving targets in various animals use as input to the fixation controller the position, the velocity and partly also the acceleration of the target's retinal image (Land & Collett 1974; Collett & Land 1975; Reichardt & Poggio 1976; Virsik & Reichardt 1976; Rossel 1980; Lisberger *et al.* 1987; Land 1992; Krauzlis & Stone 2003). In previous studies on chasing behaviour of various fly species, it has been proposed that the fixation controller relies on both retinal position of the target and on the direction of its motion. Whereas the position system is assumed to induce turns toward targets in the lateral visual field (Srinivasan &

Bernard 1977), targets in the frontal field of view are assumed to be processed by a motion-sensitive system (Land & Collett 1974; Wehrhahn *et al.* 1982; Wagner 1986). However, model simulations suggest that only one visual cue, i.e. either retinal position of the target (Cliff 1992) or retinal motion (Missler & Kamangar 1995), is sufficient to explain many aspects of chasing behaviour of the simulated fly species.

Although blowflies tend to change their flight direction during spontaneous flights by brief and rapid body saccades (Schilstra & Van Hateren 1998, 1999), flies are also able to change their flight direction gradually when following a moving target (Boeddeker *et al.* 2003). In this respect, the viewing strategies of blowflies are reminiscent of those of primates (Carpenter 1988). For convenience, we used a sinusoidal transfer function to transform retinal position into rotational velocity. Other functions are likely to lead to similar results, as long as two conditions are met: (i) the induced rotational velocity needs to increase with increasing error angle up to a certain retinal position; and (ii) to avoid a discontinuity in the posterior field of view which would reduce the stability of fixation control,

the induced rotational velocity needs to decrease for targets at more lateral retinal positions. As will be shown in a subsequent paper, saccadic tracking, as can be observed in real flies pursuing conspecifics (Wagner 1986), can be explained as an emergent property of this type of fixation control even when implementing only a smooth pursuit system into the virtual blowfly. Although the fixation controller relies exclusively on retinal target position, so far, the performance of the virtual blowfly might be improved by additionally taking into account the target's retinal velocity (Land 1992). This can be expected, at least, if the target moves like real blowflies on more complicated tracks than the circular ones used in our behavioural systems analysis (Boeddeker *et al.* 2003).

(ii) Control of forward speed

The speed controller of the virtual blowfly does not estimate its distance to the target explicitly, but uses the retinal size of the target as relevant input variable. In this regard our virtual blowfly is similar to the artificial hoverfly proposed by Cliff (1992). These simple mechanisms thus confound targets of different absolute size. Hence, targets of different absolute size will lead at different distances to a given speed of the virtual blowfly, similar to real blowflies (Boeddeker *et al.* 2003). However, if a target of given size moves at a higher velocity, it is followed by both the virtual and the real blowfly at a larger distance than a slowly moving target. This characteristic feature is an inevitable consequence of the shape of the speed controller's characteristic curve, and particularly its descending slope at large retinal target sizes (figure 1a).

(c) Significance of time constants in the control system

The performance of chasing blowflies can be explained if neuronal processing time and the time a steering command requires to become effective are taken into account. As a consequence of these time constants, the chasing blowfly retains its velocity for a while after the motor command for deceleration or acceleration is given. A blowfly approaching a small target may thus be able to reach the target and to catch it before deceleration gets too large. By contrast, when approaching a large target, deceleration is initiated at a large distance, though, at the same retinal target size as in the case of a small target. As a consequence, deceleration may become effective too early and the target is followed without being caught. The blowfly is 'trapped' by its control system. This feature can explain why large targets are caught less frequently than small ones.

(d) The potential neuronal substrate of chasing behaviour

Male-specific neurons in the fly's brain are the most likely substrate mediating chasing behaviour (Hausen & Strausfeld 1980; Zeil 1983; Gilbert & Strausfeld 1991). On the whole, the characteristics of the chasing control system that were derived on the basis of behavioural experiments and tested in the present study are in accordance with what is known about the properties of these neurons. Most male-specific neurons receive input from the dorso-frontal area of the retina which is used to keep the image of a conspecific centred during pursuit. Photorecep-

tors in this part of the retina have a higher spatio-temporal resolution than those in other parts of the eye (Land & Eckert 1985; Burton *et al.* 2001). The responses of some male-specific neurons depend on retinal target size (Gilbert & Strausfeld 1991; Gronenberg & Strausfeld 1991; Wachenfeld & Hausen 1994) in a similar way as does the forward speed of our virtual blowfly. Hence, these neurons may play a role in speed control. Computations similar to those proposed for the speed controller of the virtual blowfly are performed by the so-called lobula giant movement detector of locusts (Gabbiani *et al.* 1999; Rind & Simmons 1999), though in a different behavioural context (Robertson & Johnson 1993; Gray *et al.* 2001).

It is still not entirely clear whether male-specific neurons of flies are direction selective or mainly represent the retinal position of a moving target (Gilbert & Strausfeld 1991; Wachenfeld & Hausen 1994). Although the turning responses of our virtual blowfly were assumed to depend only on retinal target position and not on target velocity, this issue is not entirely clear at the behavioural level (see above).

In the next step of our analysis we are heading towards modelling the neuronal computations underlying fixation and speed control. These simulations will be based on experiments where male-specific neurons will be characterized with stimuli as seen by the blowfly in behavioural situations (see Lindemann *et al.* (2003) for an explanation of the approach).

The authors are grateful to Katja Karmeier, Roland Kern, Rafael Kurtz, Jens Lindemann and Frédérique Oddos for critically reading the manuscript. Thanks also to Vytautas Danilevičius who contributed in his student research project to an earlier version of the virtual blowfly. Supported by Deutsche Forschungsgemeinschaft (DFG).

REFERENCES

- Anderson, A. J. & McOwan, P. W. 2003 Model of a predatory stealth behaviour camouflaging motion. *Proc. R. Soc. Lond. B* **270**, 489–495. (DOI 10.1098/rspb.2002.2259.)
- Boeddeker, N., Kern, R. & Egelhaaf, M. 2003 Chasing a dummy target: smooth pursuit and velocity control in male blowflies. *Proc. R. Soc. Lond. B* **270**, 393–399. (DOI 10.1098/rspb.2002.2240.)
- Burton, B. G., Tatler, B. W. & Laughlin, S. B. 2001 Variations in photoreceptor response dynamics across the fly retina. *J. Neurophysiol.* **86**, 950–960.
- Carpenter, R. H. S. 1988 *Movements of the eyes*, 2nd edn. London: Pion.
- Cliff, D. 1992 Neural networks for visual tracking in an artificial fly. In *Towards a practice of autonomous systems: Proc. 1st European Conf. on Artificial Life (ECAL 91)* (ed. F. J. Varela & P. Bourguine), pp. 78–87. Cambridge, MA: MIT Press.
- Collett, T. S. & Land, M. F. 1975 Visual control of flight behaviour in the hoverfly *Syriza pipiens* L. *J. Comp. Physiol.* **99**, 1–66.
- Dickinson, M. H., Lehmann, F. O. & Sane, S. P. 1999 Wing rotation and the aerodynamic basis of insect flight. *Science* **284**, 1954–1960.
- Ellington, C. P. 1999 The novel aerodynamics of insect flight: applications to micro-air vehicles. *J. Exp. Biol.* **202**, 3439–3448.
- Gabbiani, F., Krapp, H. G. & Laurent, G. 1999 Computation of object approach by a wide-field, motion-sensitive neuron. *J. Neurosci.* **19**, 1122–1141.

- Gilbert, C. & Strausfeld, N. J. 1991 The functional organization of male-specific visual neurons in flies. *J. Comp. Physiol. A* **169**, 395–411.
- Gray, J. R., Lee, J. K. & Robertson, M. 2001 Activity of descending contralateral movement detector neurons and collision avoidance behaviour in response to head-on visual stimuli in locusts. *J. Comp. Physiol. A* **187**, 115–129.
- Gronenberg, W. & Strausfeld, N. J. 1991 Descending pathways connecting the male-specific visual system of flies to the neck and flight motor. *J. Comp. Physiol. A* **169**, 413–426.
- Hausen, K. & Strausfeld, N. J. 1980 Sexually dimorphic interneuron arrangements in the fly visual system. *Proc. R. Soc. Lond. B* **208**, 57–71.
- Juusola, M. & French, A. S. 1997 Visual acuity for moving objects in first- and second-order neurons of the fly compound eye. *J. Neurophysiol.* **77**, 1487–1495.
- Juusola, M., French, A. S., Uusitalo, R. O. & Weckström, M. 1996 Information processing by graded-potential transmission through tonically active synapses. *Trends Neurosci.* **19**, 292–297.
- Korenberg, M. J., Juusola, M. & French, A. S. 1998 Two methods for calculating the responses of photoreceptors to moving objects. *Ann. Biomed. Engng* **26**, 308–314.
- Krauzlis, R. J. & Stone, L. S. 2003 Pursuit eye movements. In *The handbook of brain theory and neural networks*, 2nd edn (ed. M. A. Arbib), pp. 929–934. Cambridge, MA: MIT Press.
- Land, M. F. 1992 Visual tracking and pursuit: humans and arthropods compared. *J. Insect Physiol.* **38**, 939–951.
- Land, M. F. & Collett, T. S. 1974 Chasing behaviour of houseflies (*Fannia canicularis*). A description and analysis. *J. Comp. Physiol.* **89**, 331–357.
- Land, M. F. & Eckert, H. 1985 Maps of the acute zones of fly eyes. *J. Comp. Physiol. A* **156**, 525–538.
- Lindemann, J. P., Kern, R., Michaelis, C., Meyer, P., Van Hateren, J. H. & Egelhaaf, M. 2003 FliMax, a novel stimulus device for panoramic and high speed presentation of behaviourally generated optic flow. *Vision Res.* **43**, 779–791.
- Lisberger, S. G., Morris, E. J. & Tychsen, L. 1987 Visual motion processing and sensory-motor integration for smooth pursuit eye movements. *A. Rev. Neurosci.* **10**, 97–129.
- Missler, J. M. & Kamangar, F. A. 1995 A network for pursuit tracking inspired by the fly visual system. *Neural Networks* **3**, 463–480.
- Reichardt, W. & Poggio, T. 1976 Visual control of orientation behaviour in the fly. I. A quantitative analysis. *Q. Rev. Biophys.* **9**, 311–375.
- Reynolds, C. W. 1999 Steering behaviors for autonomous characters. In *Game Developers Conf. 1999*, pp. 763–782. San Francisco, CA: Miller Freeman Game Group.
- Rind, F. C. & Simmons, P. J. 1999 Seeing what is coming: building collision-sensitive neurones. *Trends Neurosci.* **22**, 215–220.
- Robertson, R. M. & Johnson, A. G. 1993 Collision avoidance of flying locusts: steering torques and behaviour. *J. Exp. Biol.* **183**, 35–60.
- Rossel, S. 1980 Foveal fixation and tracking in praying mantis. *J. Comp. Physiol.* **139**, 307–331.
- Schilstra, C. & Van Hateren, J. H. 1998 Stabilizing gaze in flying blowflies. *Nature* **395**, 654.
- Schilstra, C. & Van Hateren, J. H. 1999 Blowfly flight and optic flow. I. Thorax kinematics and flight dynamics. *J. Exp. Biol.* **202**, 1481–1490.
- Srinivasan, M. & Bernard, G. D. 1977 The fly can discriminate movement at signal/noise ratios as low as one-eighth. *Vision Res.* **17**, 609–616.
- Srinivasan, M. V. & Davey, M. 1995 Strategies for active camouflage of motion. *Proc. R. Soc. Lond. B* **259**, 19–25.
- Virsik, R. P. & Reichardt, W. 1976 Detection and tracking of moving objects by the fly *Musca domestica*. *Biol. Cybern.* **23**, 83–98.
- Wachenfeld, A. & Hausen, K. 1994 The role of male-specific visual interneurons in the mating behavior of the blowfly, *Calliphora erythrocephala* (Meig.). In *Göttingen neurobiology report* (ed. N. Elsner & H. Breer), p. 440. Stuttgart and New York: Thieme.
- Wagner, H. 1986 Flight performance and visual control of flight of the free-flying house-fly (*Musca domestica* L.) II. Pursuit of targets. *Phil. Trans. R. Soc. Lond. B* **312**, 581–595.
- Warzecha, A. K. & Egelhaaf, M. 2001 Neuronal encoding of visual motion in real-time. In *Motion vision: computational, neural, and ecological constraints* (ed. J. Zeil & J. M. Zanker), pp. 239–277. Berlin, Heidelberg and New York: Springer.
- Wehrhahn, C., Poggio, T. & Bühlhoff, H. 1982 Tracking and chasing in houseflies (*Musca*). *Biol. Cybern.* **45**, 123–130.
- Zeil, J. 1983 Sexual dimorphism in the visual system of flies: the divided brain of male Bibionidae (Diptera). *Cell Tissue Res.* **229**, 591–610.

As this paper exceeds the maximum length normally permitted, the authors have agreed to contribute to production costs.